Studies in Surface Science and Catalysis 130
A. Corma, F.V. Melo, S. Mendioroz and J.L.G. Fierro (Editors)

The nature of the active species on the Fe/MgO used in the combustion of methane

R. Spretz[a], S.G. Marchetti[b], M.A. Ulla[a] and E.A. Lombardo[a]

[a] Instituto de Investigaciones en Catálisis y Petroquímica, INCAPE (FIQ, UNL-CONICET), Santiago del Estero 2829, C.P. 3000, Santa Fe, Argentina

[b] Centro de Investigación y Desarrollo en Procesos Catalíticos, CINDECA, UNLP, Calle 47 N° 257, C.P. 1900, La Plata, Argentina

A series of Fe/MgO solids (1.5-9.0 wt % Fe) calcined at 1073 K is shown to be made up of $MgFe_2O_4$ and Fe^{3+} dispersed in the MgO matrix. Mössbauer spectroscopy provided the data to quantify both species. The rate data for methane combustion correlates with the spinel content but not with the Fe^{3+} concentration. The locus of activity is discussed in terms of both the solid features and existing literature.

1. INTRODUCTION

The catalytic combustion in gas turbines allows both a better utilization of energy and the abatement of NO_x emissions. The first commercial unit installed in an electrical utility began to operate by the end of 1998 [1]. However, the catalytic problem is far from solved and new materials are needed. Berg and Järås [2] have proposed MgO as an interesting support for the combustion of methane due to its ability to develop and maintain a large surface area. Other materials with high thermal stability such as mixed oxides and particularly spinels [3] are potential candidates for this application. Along this line, the incorporation of Fe to MgO leads to a sharp increase in catalytic activity. This system has already been applied in catalysis. In the reduced form, Boudart et al. [4-6] characterized Fe/MgO employing Mössbauer spectroscopy. Fe/MgO was tested by Ueda et al. [7] for the cross-coupling reactions leading to α,β-unsaturated compounds. In this work, we investigate the nature of the active species of Fe/MgO solids using several techniques, bearing in mind its use for the high temperature combustion of methane.

2. EXPERIMENTAL

2.1. Catalyst Preparation

A series of Fe(w)/MgO catalysts (w=1.5, 3, 6 and 9 wt %) was prepared by wet impregnation adding aqueous 0.5 M $Fe(NO_3)_3 . 9H_2O$ solutions to a suspension of MgO in distilled water. The resulting slurry was intensely stirred on a hot plate until dryness.

The solid so obtained was kept in an oven at 380 K overnight. Finally, it was calcined in air flow at 1073 K for 10 h. An aliquot of the support was also calcined under the same conditions. The model $MgFe_2O_4$ solid was also synthesized.

2.2. Catalyst Characterization

The X-ray diffraction patterns were acquired using an XD-D1 Shimadzu instrument with monochromator employing CuK_α radiation. The Raman spectra were obtained using a JASCO TRS-600SZ-P spectrophotometer. The excitation source was the 514.5 nm line of a Spectra 9000 Photometrics Ar ion laser. The Mössbauer spectra were acquired at 298 and 16 K with a standard 512-channel spectrometer with transmission geometry. A ^{57}Co in Rh matrix source of nominally 50 mCi was used. Velocity calibration was performed against a 6 μm thick α-Fe foil.

2.3. Catalytic Measurements

The catalytic activity of Fe(w)/MgO for methane combustion was measured using a quartz microreactor operated in plug flow mode. A sample of 0.050 g with a particle size between 60-80 mesh was used for each test. CH_4, O_2 and N_2 in variable proportions were fed using mass flow controllers. The typical hourly space velocity was 480.000 h^{-1}. The analysis of the reacting stream was carried out using an on-line chromatograph equipped with a Porapak Q column and a TCD.

3. RESULTS

3.1. Catalyst Characterization

The XRD patterns of the catalysts show the MgO reflections and three weaker signals assigned to $MgFe_2O_4$, which increase in strength at higher Fe contents. Comparing the diffractograms of the Fe/MgO series with the ones corresponding to $MgFe_2O_4$, we can conclude that the catalysts are made up of spinel and MgO only. Let us see what Raman and Mössbauer spectroscopies can show us about this system.

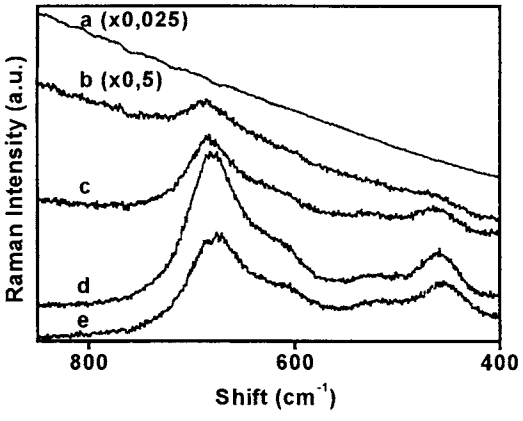

Figure 1. Raman spectra of Fe(w)/MgO catalysts, from (a) to (d): w = 0; 3; 6 and 9 wt %, and (e): $MgFe_2O_4$.

The Raman spectra of the catalysts show the characteristic bands of $MgFe_2O_4$ at 714, 542 and 472 cm^{-1} (Fig. 1). The support, just like the sample with 1.5 % Fe content (not shown), does not present Raman signals but fluorescence (that's why it was attenuated by a factor of 40). The fluorescence diminishes in Fe(6%)/MgO and almost disappears in the solid with 9%. This fluorescence

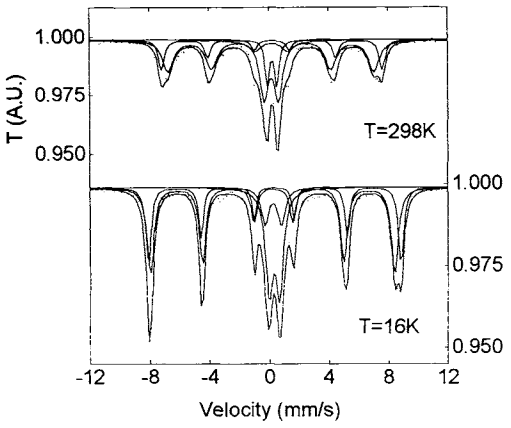

Figure 2. Mössbauer spectra of Fe(6)/MgO showing the central doublets (Fe^{3+} dispersed in MgO) and the sextuplets (Fe^{3+} in $MgFe_2O_4$) present in the series.

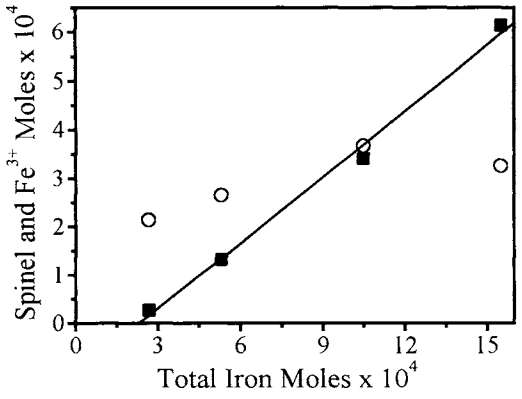

Figure 3. $MgFe_2O_4$ (■) and Fe^{3+} (○) amounts in the Fe/MgO catalysts as a function of the total iron load, calculated from the Mössbauer spectra (sample weight 1 g).

may be due to the terminal hydroxyls of MgO.

The Mössbauer spectra of Fe/MgO at room temperature are made up of a doublet and a sextuplet in every case. At 16 K, it is possible to discriminate the contribution of the Fe^{3+} sextuplets located at the tetrahedral and octahedral spinel positions. Figure 2 shows the spectra corresponding to Fe(6)/MgO. At low temperature the superparamagnetic relaxation is eliminated since the slightly parabolic background, present at 298 K, has disappeared. Besides, the ratio of the sextuplet/doublet areas does not change when the temperature is lowered from 298 to 16 K. Therefore, the possibility that doublets at 16 K are due to tiny crystals of $MgFe_2O_4$ and/or α-Fe_2O_3 can be discarded. This, together with the fact that the Mössbauer parameters for the doublets are almost identical in all samples, led us to assign the doublets to Fe^{3+} located in the MgO holes. The number of intersticial Fe^{3+} and $MgFe_2O_4$ moles per gram of catalyst was calculated using the Mössbauer data (Figure 3). Note that the amount of Fe^{3+} stays essentially constant while the spinel amount increases by a factor of 23. This seems to indicate that at low iron concentrations, finely Fe^{3+} dispersion takes place and as the iron loading increases above ca. 1%, the spinel phase starts to develop. The next question is which iron-containing phase is the active one. This question will be answered after the kinetic data have been presented.

3.2. Catalytic measurements

Figure 4 shows the raw kinetic data against the $MgFe_2O_4$ content in the catalysts, in the 848-948 K temperature range. In these experiments, the reactant concentration was as follows: CH_4 = 2% v/v; O_2 = 8% v/v, balance N_2. A saturation

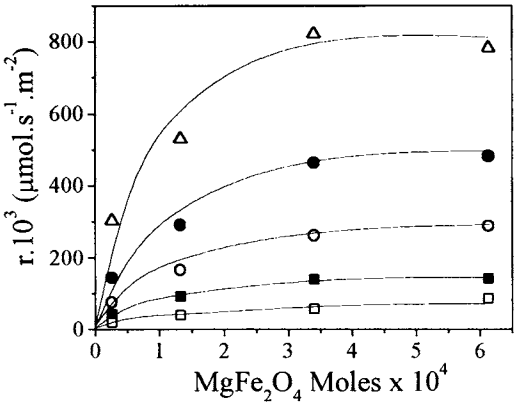

Figure 4. Effect of the spinel amount (sample weight 1 g) upon the reaction rate for the combustion of methane at (□) 848, (■) 873, (○) 898, (●) 923 and (△) 948 K.

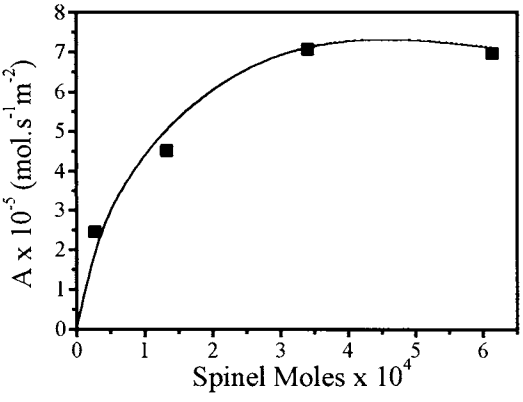

Figure 5. Effect of the spinel content upon the preexponential factor of the surface reaction rate constant (sample weight 1 g).

value was achieved at every temperature when the total iron content was 6% or more. No correlation was obtained when the same plot was made against the Fe^{3+} concentration. The spinel was also catalytically tested. This model compound had a low surface area; therefore, a low space velocity at 948 K was used. Under these conditions the rate obtained agreed within 10% with the saturation value reported in Fig. 4.

The results described below correspond to the Fe(6)/MgO sample. The same trend was observed for the other catalysts. The combustion rate presents a Langmuir-Hinshelwood dependence with both methane and oxygen concentration. The apparent order for methane varied between 0.60 and 0.86 while that for oxygen covered a range between 0.43 and 0.83.

Thus, the reacting system can be modelled as follows:

$$CH_{4\,(g)} + S_1 \overset{K_1}{\rightleftharpoons} CH_{4\,(ads)} \qquad (1)$$

$$O_{2\,(g)} + S_2 \overset{K_2}{\rightleftharpoons} O_{2\,(ads)} \qquad (2)$$

$$CH_{4\,(ads)} + O_{2\,(ads)} \overset{k}{\longrightarrow} {\bullet}CH_{3\,(g)} + HO_2{\bullet}_{(g)} \qquad (3)$$

Paths (1) and (2) correspond to the adsorption equilibrium of both reactants on two different sites. Path (3) is considered to be the rate-limiting step in this scheme. This mechanism leads to the following expression for the reaction rate:

$$r_{CH_4} = k \cdot \theta_{CH_4} \cdot \theta_{O_2} = k \cdot \frac{K_1 \cdot \bar{p}_{CH_4}}{1 + K_1 \cdot \bar{p}_{CH_4}} \cdot \frac{K_2 \cdot \bar{p}_{O_2}}{1 + K_2 \cdot \bar{p}_{O_2}} \qquad (4)$$

Such an expression was already proposed by Berg and Järås [2] over MgO. Although the expression of the reaction rate is the same, note that in the conditions employed in this work, the support itself is inactive for this reaction.

The temperature dependance of the surface reaction is given by $k = A.\exp(-E_c / RT)$, where A is a function of the active site concentration. This parameter is then a good candidate to explore correlations with both spinel and Fe^{3+} concentrations. By processing the data for all the catalysts, first K_1 and K_2 as a function of temperature, and then E_c and A were calculated.

Figure 5 shows the variation of the preexponential factor A with the amount of spinel present per gram of catalyst. No correlation develops when the Fe^{3+} concentration is used in the abscissa (not shown). These results are also consistent with the assignment of the active phase to $MgFe_2O_4$.

4. DISCUSSION

XRD analysis and the Raman spectra confirmed the formation of the $MgFe_2O_4$ spinel on the Fe/MgO series. However, the Mössbauer spectroscopy completed the overall picture of the solid structure, giving us the data to quantify the different iron species. Boudart et al. [4] studied the same system in its reduced form using the Mössbauer spectroscopy. They found Fe^{2+} clusters in MgO whose concentrations varied only a little with the iron loading. In agreement with our results, Fe cations tend firstly to form a solid solution with the magnesium oxide before forming the spinel phase, after reaching a given concentration.

Asakura and Iwasawa [8] characterized the Fe/MgO system in its oxidized form. They suggested the existence of coordinatively unsaturated basic O^{2-} sites and acidic Fe^{3+} sites in the Fe/MgO system at the interface between $MgFe_2O_4$ and the parent MgO lattice. With our technique, we cannot distinguish the location of the Fe^{3+} inserted in the MgO lattice. However, the insertion of Fe^{3+} is favored by the existence of Mg^{2+} vacancies which are more apt to occur at the interface between $MgFe_2O_4$ and MgO. Thus, it is likely that a large proportion of the detected Fe^{3+}-MgO is located at the said interface.

The rate data correlates with the amount of spinel present in the catalyst. However, the rate reaches a saturation value with increasing spinel concentration (Fig. 4). The most straightforward explanation for the catalytic behavior of the Fe/MgO series with iron concentration, namely the complete coverage of the catalyst surface with the active site, is supported neither by the SEM micrographs nor by the Electron Probe Microanalysis (EPM) data (not shown). They reveal that even the 9 wt % Fe catalyst contains islands of MgO decorating the catalyst surface. There is also a significant surface heterogeneity in the whole series. The origin of the MgO islands is discussed below.

The equilibrium system in aqueous solution was solved for the conditions prevailing after the addition of the Fe nitrate solution to the magnesium hydroxide suspension [9]. The calculations show that during the impregnation process the total precipitation of the Fe^{3+} cation takes place. At the same time, in order to satisfy the

electrical neutrality (presence of the nitrate anions) an equivalent amount of Mg^{2+} migrates into the solution. During the drying process, a final deposition of $Mg(NO_3)_2$ on the solid takes place. In the calcination stage, the former becomes MgO partially covering the impregnated Fe, thus forming islands on the catalyst.

At this point, it is possible to speculate about the nature of the active sites. Since the kinetic data do not correlate with the concentration of the Fe^{3+} dispersed in MgO, this phase cannot be considered as an active one. On the other hand, the $MgFe_2O_4$ model compound behaves similarly to the supported catalysts with 6% or more o iron. This, together with the correlation observed between rates and spinel content indicate that the loci of active sites are located on the $MgFe_2O_4$ phase.

5. CONCLUSIONS

In the Fe/MgO system Fe^{3+} cations are finely dispersed in the MgO matrix at low Fe content (ca. below 1 wt %) while at higher metal concentrations, the $MgFe_2O_4$ spinel phase develops. From about 1 wt % up to 9 wt % Fe, the spinel concentration increases 20 times, while the Fe^{3+} concentration remains essentially constant.

The plateaus observed in Figures 4 and 5 cannot be explained by the complete surface coverage with active species. The formation of MgO islands on the catalyst surface takes place, thus leading to an important heterogeneity, inherent to the preparation method.

The kinetic results are consistent with the participation of two different active sites. They must be located on the $MgFe_2O_4$ spinel phase.

ACKNOWLEDGMENTS

The authors wish to acknowledge the financial support received from CONICET, ANPCyT and UNL (CAI+D '96). Thanks are also given to the Japan International Cooperation Agency (JICA) for the donation of the equipment, and to Elsa Grimaldi for her help in the English edition of the manuscript.

REFERENCES

1. XONON Systems, catalytica.inc.com, October 8, 1998.
2. M. Berg and S. Järås, App. Catal. A: General **114** (1994), 227.
3. D.L. Trimm, Catal. Today, **26** (1995) 231.
4. M. Boudart, A. Delbouille, J.A. Dumesic, S. Khammouna and H. Topsøe, J. Catal. **37** (1975) 486.
5. J.A. Dumesic, H. Topsøe, S. Khammouma and M. Boudart J. Catal. **37** (1975) 503.
6. J.A. Dumesic, H. Topsøe and M. Boudart, J. Catal. **37** (1975) 513.
7. W. Ueda, T. Yokoyama, Y. Moro-Oka, and t. Ikawa, Ind. Eng. Chem. Prod. Res. Dev., **24** (1985) 340.
8. K. Asakura and Y. Iwasawa, Mat. Chem. Phys. 18 (1988) 499.
9. R.Spretz, Ph.D. Thesis, Universidad Nacional del Litoral, Argentina (1998).